

Final Year Dissertation
Degree in Biochemistry and Molecular Biology

Cholinergic neurons within the nucleus basalis magnocellularis in bilaterally lesioned rats with 192IgG-saporin

Author:
Leyre Merino Galán
Co-director:
Alberto Llorente Ovejero
Director:
Rafael Rodríguez-Puertas

Keywords: Alzheimer's disease, acetylcholine, nucleus basalis magnocellularis, 192IgG-saporin.

INDEX

1. Introduction	3
2. Objectives	5
3. Materials and methods	5
3.1. Animals	5
3.2. Reactives, drugs and solutions	5
3.3. Stereotaxic surgery and immunotoxin injection	6
3.4. Tissue handling	6
3.5. AChE enzyme histochemistry	7
3.6. Quantification	7
3.6.1 AChE ⁺ neuron density	7
3.6.2 AChE activity	8
3.7. Statistical analysis	8
4. Results	9
4.1. AChE⁺ neuron density	9
4.2. AChE activity	10
4.3. Correlation between AChE⁺ neuron density and AChE activity	12
5. Discussion	13
6. Bibliography	14

1. Introduction

Alzheimer's disease (AD) is a neurodegenerative disorder manifested by cognitive and memory decline and progressive impairment of daily activities and diverse neuropsychiatric symptoms and behavioural dysfunctions. According to the histopathological and neurochemical alterations, the AD is characterized by a neuronal degeneration and the loss of synapses, as well as the accumulation of senile plaques composed mainly of β -amiloid protein and neurofibrillary tangles formed by hyperphosphorilated tau protein [1, 2, 3]. Approximately 5-10% of cases are considered hereditary according to the different gene mutations associated to this disorder. Mutations in the genes APP, PSEN1 and PSEN2 are related to the early-onset familial AD, while mutations in the APOE, which encodes the apolipoprotein E, are related to the late-onset familial AD [4].

AD is considered a serious global health problem with an increasing prevalence that affects approximately to almost the 50% of elders over 85 years. Therefore, prevalence studies suggest that 24.3 million people suffer from AD worldwide, and that number is projected to increase accordingly with the increase in life expectancy [5]. Despite this serious fact, and although current management with cholinesterase (AChE) inhibitors and NMDA-receptor antagonists produces moderate symptomatic improvement at best, the fact is that no effective treatment exists for the AD [6]. Novel therapeutic options are therefore needed.

As the etiopathology of the Alzheimer disease is still unknown, many hypotheses about this pathology have been proposed. The AChE inhibitors were developed according to the cholinergic hypothesis, which postulates that the loss or dysfunction of the cholinergic neurons within the basal forebrain, contribute to memory impairment in both, nonpathological aging and in AD patients where the loss of these neurons is more severe [1]. Although there is a widespread decline in other neurotransmitter-containing cell bodies in end-stages, the most consistent losses throughout the progression of AD are seen in long projecting neurons, including cholinergic neurons of the basal forebrain [7]. Thus, further investigations about the basal forebrain cholinergic system (BFCS) and its projections, related to the modulation of cognitive functions are necessary. The BFCS consists of the cholinergic neurons distributed rostro-caudally in four main groups that are; the medial septum, both the vertical and horizontal limbs of the diagonal band of Broca and the nucleus basalis magnocellularis (nbM; homologous to the nucleus basalis of Meynert in primates and human brain) [8]. BFCS is considered one of the brain systems with the longest projections and the involvement of the cholinergic system in AD has been extensively documented. The nbM and medial septum provide widespread cholinergic innervations to the entire cortex and hippocampus,

respectively. These pathways play a key role in cognitive processes such as learning, memory and attention. In fact, loss of BFCS neurons in AD patients results in a reduction in acetylcholine (ACh) levels in projecting areas, leading to the characteristic symptoms of this disease [9, 10, 11]. The cholinergic system can be analyzed by choline acetyltransferase (ChAT) and acetylcholinesterase (AChE) biomarkers.

Both, *in vivo* and *in vitro* approaches of BFCS lesion have been used to mimic the cholinergic degeneration described in AD. The first studies developed to lesion the BFCS included mechanical lesions such as nerve tracts transections which lead to retrograde degeneration of cholinergic neurons, but they were not selective. Other studies were conducted by inducing locally electrolytic or radiofrequency lesions, but caused non-specific cell damage. Later, the use of neurotoxic excitatory amino acids (NEEAs) such as kainic, ibotenic and quisqualic acid became popular to induce the brain lesions. In fact, chemical lesions with NEEAs have been found to be more selective than electrolytic or radiofrequency lesions as they specifically eliminate the neurons of interest without affecting other types of cells. Many of these NEEAs are potent selective agents at glutamate receptors that destroy cells bearing these receptors by high excitation or calcium ion overload. However, many different types of cells bear glutamate receptors and, although cholinergic neurons are vulnerable to these toxins, other cell types, mainly GABAergic neurons, are destroyed when NEEAs are infused into the nbM. The ethylcholine aziridinium ion (AF64A) was developed to delete cholinergic neurons specifically since it targets a specific membrane protein present on cholinergic terminals, the high-affinity choline transporter. Nevertheless, the specificity of this alkylating agent for cholinergic neurons *in vivo* was difficult to ensure because of the high reactivity of the aziridinium ion. The discovery and introduction of the use of 192IgG-saporin, a highly specific cholinergic immunotoxin, have allowed to improve the methodology related to the study of the consequences of the cholinergic damage. The immunotoxin consists of the monoclonal antibody 192IgG coupled to saporin by a disulfide bridge. Saporin is a derivative obtained from the plant *Saponaria officinalis*. The specificity of this toxin is due to the antibody component which is directed against the rat p75^{NTR} receptor, a low-affinity neurotrophin receptor protein mainly expressed in basal forebrain cholinergic neurons. Following receptor binding and internalization, the immunotoxin enzymatically inactivates the large ribosomal subunit, thereby blocking protein synthesis and ultimately resulting in cell death. Its specificity makes 192IgG-saporin a useful tool to lesion BFCS, mimicking the AD-associated cholinergic decline [12, 13, 14]. Although different areas of the BFCS are affected in AD patients, the most affected area is the nbM. The degeneration of the nbM and its consequent loss of innervations

have been demonstrated to mimic the cholinergic and cognitive decline seen in AD [15], but the etiopathogenesis of the neurodegeneration remains being a mystery.

2. Objectives

1. To optimize the *in vivo* model of nbM lesion by the intraparenchymal administration of the 192 IgG-saporin immunotoxin.
2. To optimize the AChE staining method for the quantification of cholinergic fibers in the projection areas.
3. Demonstrate the selective loss of AChE positive neurons (AChE⁺) in the nbM after the *in vivo* administration of the immunotoxin to rats.
4. Analyze by densitometry the effect of the specific cholinergic lesion on different brain areas innervated by the nbM.
5. Study the different correlation between AChE⁺ neurons at the nbM and AChE activity in the different brain areas.

3. Materials and methods

3.1. Animals

Adult male (250-300 g) Sprague-Dawley rats were obtained from the animal facilities of the University of the Basque Country (UPV/EHU). The experimental procedures involving the participation of animals were carried out in strict accordance with the current legislation requirements with the approval of the Institutional Animal Welfare Ethical Committee (CEBA). Animals were maintained under standard housing conditions and kept on a normal diet and tap water *ad libitum* with 12-h light cycle.

The animals were divided in three groups.

- Injection simulation without administration (SHAM-operated; $n=6$)
- Artificial cerebrospinal fluid stereotaxic administration (CSF; $n=14$)
- 192IgG-saporin stereotaxic administration (192IgG-SAP; $n=25$)

3.2. Reactives, drugs and solutions

- CSF: NaCl 0.148 M, KCl 2.7 mM, MgCl₂ · 6H₂O 0.85 mM and CaCl₂ 1.2 mM, pH 7.4.
- PBS: 0.1 M, pH 7.4.
- Tris-Maleate: 0.1 M, pH 6.0.

- AChE reaction buffer: 0,1 M Tris-Maleate pH 6.0, 5 mM sodium citrate, 3 mM CuSO_4 , 0,1 mM ISO-OMPA, 2 mM acetylthiocholine iodide and either 0,5 mM or 5 mM $\text{K}_3\text{Fe}(\text{CN})_6$.
- Fixative solution: 4% paraformaldehyde in 0.1 M PBS.
- Anaesthesia: Ketamine (100 mg/kg) and Xilazine (10 mg/kg).
- Antibiotic: Oxitetracilin (2.25 mg/kg).
- Immunotoxin: 192IgG-Saporin (Millipore, Temecula, CA) dissolved in CSF.

All the reagents and drugs were of the highest commercially available quality for the necessity of the studies.

3.3. Stereotaxic surgery and immunotoxin injection

Animals were deeply anesthetized and placed on a Kopf stereotaxic frame. A surgical longitudinal incision was made to the skin overlying the skull to localize the “Bregma” and “Lambda” cranial sutures. A hole was made through the skull with a dental drill according to the stereotaxic coordinates of the nbM obtained from the atlas Paxinos and Watson [16]: +1,5 mm antero-posterior from “Bregma”, ± 3 mm latero-dorsal from medial line and +7,8 mm depth from the cranial surface. The administration was made with a micro syringe coupled to an automatic pump, control animals received 1 μL of artificial cerebrospinal fluid solution in each hemisphere in a constant rate of 0,3 $\mu\text{L}/\text{min}$, while treated animals received 1 μL of 192IgG-Saporin (130 ng/ μL). The needle was left in place for an additional 5 min after the administration in order to guarantee a correct diffusion and avoid reflux. We have used a new 33 gauge needle for stereotaxic administrations in the brain (Neuros TM Syringe) to minimize the damage. Regarding the SHAM-operated group, it was operated in a similar way, but no liquid was injected. After the wound was cleaned and closed with sterile thread, an intramuscular dose of antibiotic was administered and the animals were returned to their cages.

3.4. Tissue handling

8 days after the intraparenchymal injection into the nbM, the animals were deeply anesthetized. One animal of each group was used to obtain fixed tissue and the rest to obtain fresh tissue. Two different protocols were carried out in order to obtain the cerebral samples.

- *Fresh Tissue*: following the anesthesia the animals were decapitated and the brains were carefully removed and immediately frozen at -80°C .
- *Fixed Tissue*: the animals were deeply anesthetized as above mentioned and were transcardially perfused with 75 ml of 0.1 M PBS with 0.1% heparine (37°C)

followed by cold (4°C) 350 ml of fixative solution. The brains were carefully removed and post-fixed by immersion in the same fixative solution for 90 min. The tissue was cryoprotected in 20% sucrose solution in 0.1 M PBS for 24 h and frozen by immersion in isopentane at -80°C.

The brains were cut using a cryostat (-20°C) and 20 µm thick serial coronal sections of the basal forebrain in the level of medial septum (MS) and nbM and also dorsal (DHC) and ventral (VHC) hippocampus were obtained and mounted on gelatine-coated slides.

3.5 AChE enzyme histochemistry

For the identification of AChE⁺ neurons in the nbM and detection of AChE activity in the projection areas, a slightly modified method of Karnovsky and Roots (1968; [17]) was used. First, brain sections from the three different groups of animals were dried at room temperature (RT) (20') and washed twice in 0.1 M PBS, pH 7.4 (10'). Fresh tissue sections were post-fixed in fixative solution in PBS 0.1 M (30') and briefly dipped in 0.1 M Tris-Maleate, pH 6.0, to eliminate the fixative. Fresh or fixed tissues were preincubated twice in 0.1 M Tris-Maleate, pH 6.0 (2x10'). Following, sections were incubated in reaction buffer in the dark with constant and gentle agitation on a rotating platform in order to facilitate the AChE activity-reaction described in *Figure 1*. To optimize the AChE staining protocol, the incubation times varied from 10 to 30 min and from 80 to 110 min. The objective was to stain cholinergic neurons in the nbM or to identify cholinergic fibers in the projection areas, respectively. Enzymatic reaction was stopped in 0.1 M Tris-Maleate, pH 6.0, at RT (2x10'). Sections were dehydrated with increasing concentrations (%) of ethanol. H₂O_d (10'), 50% (10'), 75% (5'), 96% (5') and 100% (5') and covered with di-n-butyl phthalate in xylene (DPX).

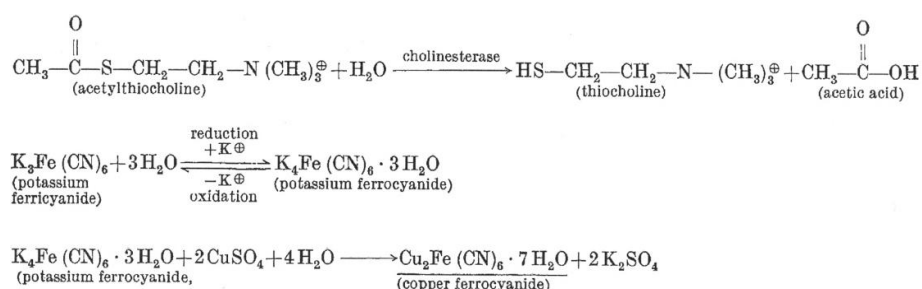


Figure 1: Reaction sequence for the production of copper ferrocyanide through cholinesterase activity [18].

3.6 Quantification

3.6.1 AChE⁺ neuron density:

Representative microphotographs of fresh tissue were obtained using a camera connected to a Zeiss microscope with the SPOT Advanced TM software. AChE⁺ neurons were

counted using ImageJ software in 10x magnification images. Both hemispheres were analyzed in the administration area ("lesion"; +1.5 mm antero-posterior from Bregma) or in the surrounding area ("adjacent to lesion"; +1 mm; +2 mm antero-posterior from Bregma) for the 3 groups of animals (SHAM-operated, CSF, 192IgG-SAP). Considering that the nbM is 1 mm width and each section is 20 μM thick, 50 cuts must be done to analyze the whole nbM. Hence, the mean value of AChE positive cells per mm^2 was multiplied by 50 to obtain the number of cells per mm^3 at the nbM.

3.6.2 AChE activity

To evaluate the cholinergic damage induced by 192IgG-saporin, the optical density of AChE⁺ nerve fibers was measured in the nbM projection areas. Fresh tissue sections were scanned at 24bits, 600 pixels/inch resolution and images were converted to 8-bit for the optical density quantification in the CSF and 192IgG-SAP groups. Fixed tissue was microphotographed at 20x and 40x magnification for the detailed images. The optical density for the AChE staining was analyzed using NIH (Image J) software. A quantitative analysis of the AChE activity was measured in different brain areas, such as cortex (cingular, motor, somatosensory, piriform and entorhinal), hippocampus (CA1 pyramidal, molecular layer (Lmol), radiatum layer (Rad), CA2 pyramidal, CA3 pyramidal, granular dentate gyrus (grDG), and molecular dentate gyrus (molDG)) and amygdala (anterior, lateral, basolateral, central and medial). The optical density level of the background for each section was measured and subtracted to the values of each brain area to obtain the net optical density. The net values obtained for the different projection areas were compared between CSF and 192IgG-SAP groups.

3.7. Statistical analysis

A multiple statistical analysis was performed to compare the density of AChE⁺ neurons (AChE⁺ neurons/ mm^3) between the 3 groups of treatment. A normality test was carried out (Shapiro-Wilk) to test if the values come from a Gaussian distribution. One way analysis of the variance (ANOVA) followed by Bonferroni's post-hoc test was used when data followed a Gaussian distribution or Kruskal-Wallis analysis followed by Dunns post-hoc test when were non-normal data. The AChE optical density (CSF vs. 192IgG-SAP data), were analyzed using an unpaired student "t" test. Data were expressed as mean \pm SEM. To analyze a possible correlation between AChE⁺ neuron density (AChE⁺ neuron/ mm^3) and AChE activity, Pearson's analysis was used. Statistical analyses were performed using GraphPad 3.0. Changes were considered statistically significant if $p < 0.05$.

4. Results

4.1 AChE⁺ neuron density

The cholinergic neuron density into the nbM was measured by using the AChE reaction staining. We observed no differences between the SHAM-operated and CSF groups. Nevertheless, we found statistically significant differences between both the SHAM-operated and CSF groups when compared to the 192IgG-SAP group (*Figure 2*).

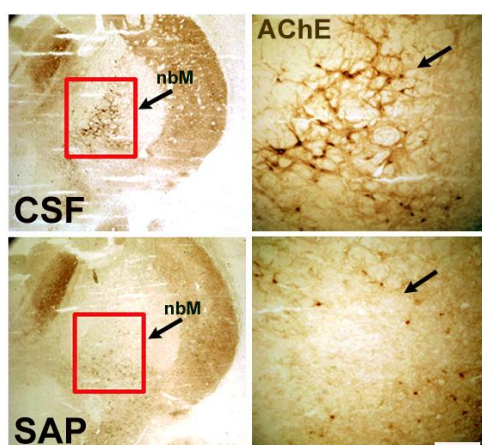


Figure 2: Microscope images corresponding to a representative CSF rat (above row) and 192IgG-SAP (below row) brain slices stained using the AChE reaction. Note the effect of 192IgG-saporin administration in the cholinergic neuron density in the nbM (red square). Control rats (CSF) exhibited a high density of AChE⁺ neurons in the nbM, but rats lesioned with 192IgG-saporin displayed a dramatically reduced number of AChE⁺ neurons. Scale bar = 100 μ m.

The estimated number of AChE⁺ neurons (cells/mm³) in the nbM of the CSF, SHAM-operated and 192IgG-SAP groups were 981 ± 63 , 999 ± 111 and 151 ± 24 , respectively. We also analyzed the effect of the immunotoxin in an adjacent area of the lesion and the density of AChE⁺ neurons was 357 ± 34 . The differences in the number of AChE⁺ neurons between the groups are represented in *Figure 3*.

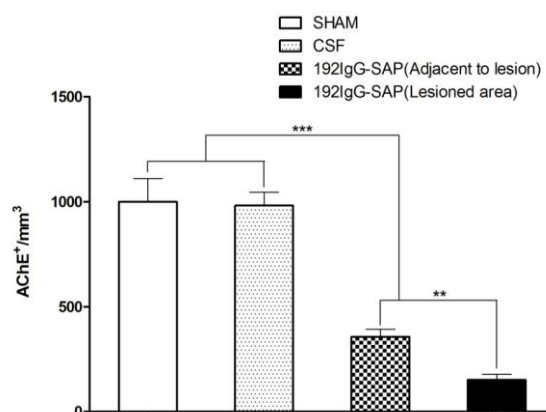


Figure 3: Quantitative analysis of AChE⁺ neuron density of the different groups: SHAM-operated, CSF and 192IgG-SAP in the injection area and adjacent to the lesion. One-way ANOVA followed by Bonferroni's test. ** $p < 0.01$ vs. 192IgG-SAP (lesioned area); *** $p < 0.001$ vs. 192IgG-SAP (lesioned area and adjacent to the lesion).

4.2 AChE activity

In order to optimize the previous AChE histological staining, different incubation times were performed from 80 to 110 min, and different concentrations of $K_3Fe(CN)_6$ were also used. For all groups of rats, optimal results for optical density measurements were obtained with an incubation time of 80 min and 0.5 mM of $K_3Fe(CN)_6$. The 192IgG-saporin injection induced a reduction of the cholinergic fiber densities at the cortical, hippocampal and amygdaloid areas that are innervated by the cholinergic cells of the nbM (*Table 1*). These reductions were significant for all the analyzed cortical areas; CA3 (pyramidal) and dentate gyrus (granular) of the hippocampus; and anterior, lateral and medial regions of the amygdala (*Figure 4 and Figure 5*).

Table 1: Quantitative analysis of AChE activity (optical density; a.u.) at the analyzed projection areas of the nbM. Data are represented as mean value \pm SEM.

	AChE activity		
	CSF (n=11)	192IgG-SAP (n=12)	Δ %
Cortex			
Cingular	31.7 \pm 1.3	25.6 \pm 1.0*	-19.2%
Motor	24.5 \pm 0.8	8.4 \pm 0.5***	-65.8%
Somatosensory	27.2 \pm 1.1	8.0 \pm 0.6***	-70.8%
Piriform	39.4 \pm 1.7	33.5 \pm 1.4***	-14.9%
Entorhinal	29.0 \pm 1.4	17.7 \pm 1.0*	-38.9%
Hippocampus			
CA1 (Pyramidal)	57.0 \pm 1.3	53.0 \pm 1.8	-7.1%
Lacunosum moleculare	12.8 \pm 0.9	13.3 \pm 0.5	4.4%
Radiatum layer	21.1 \pm 0.8	19.9 \pm 0.6	-5.6%
CA2 (Pyramidal)	74.7 \pm 1.9	69.6 \pm 2.2	-6.9%
CA3 (Pyramidal)	59.5 \pm 1.4	53.1 \pm 2.2*	-10.7%
Dentate gyrus (granular)	63.3 \pm 2.3	54.5 \pm 2.2*	-13.9%
Dentate gyrus (moleculare)	36.9 \pm 1.3	35.0 \pm 1.3	-5.2%
Amygdala			
Anterior	81.8 \pm 5.3	56.7 \pm 2.4***	-30.7%
Lateral	59.2 \pm 4.4	44.9 \pm 1.7**	-24.1%
Basolateral	117.7 \pm 4.4	103.1 \pm 3.6	-12.4%
Central	30.5 \pm 1.7	26.6 \pm 1.2	-12.6%
Medial	22.1 \pm 1.9	15.4 \pm 1.0*	-30.5%

Student "t" test. CSF vs. 192IgG-SAP. *p<0.05; **p<0.01; ***p<0.001.

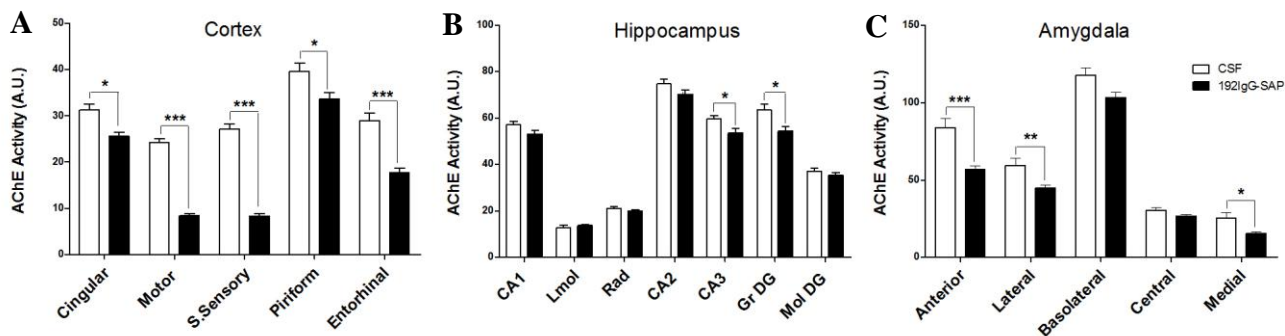


Figure 4: Quantitative representation of AChE activity at the analyzed projection areas of the nbM. Cortex (A), hippocampus (B) and amygdala (C). Note the significant decrease in the density of cholinergic innervation at cortical areas that was more moderated at some of the hippocampal and amygdaloid subareas. Student “t” test CSF vs. 192IgG-SAP. * $p < 0.05$; ** $p < 0.01$; *** $p < 0.001$.

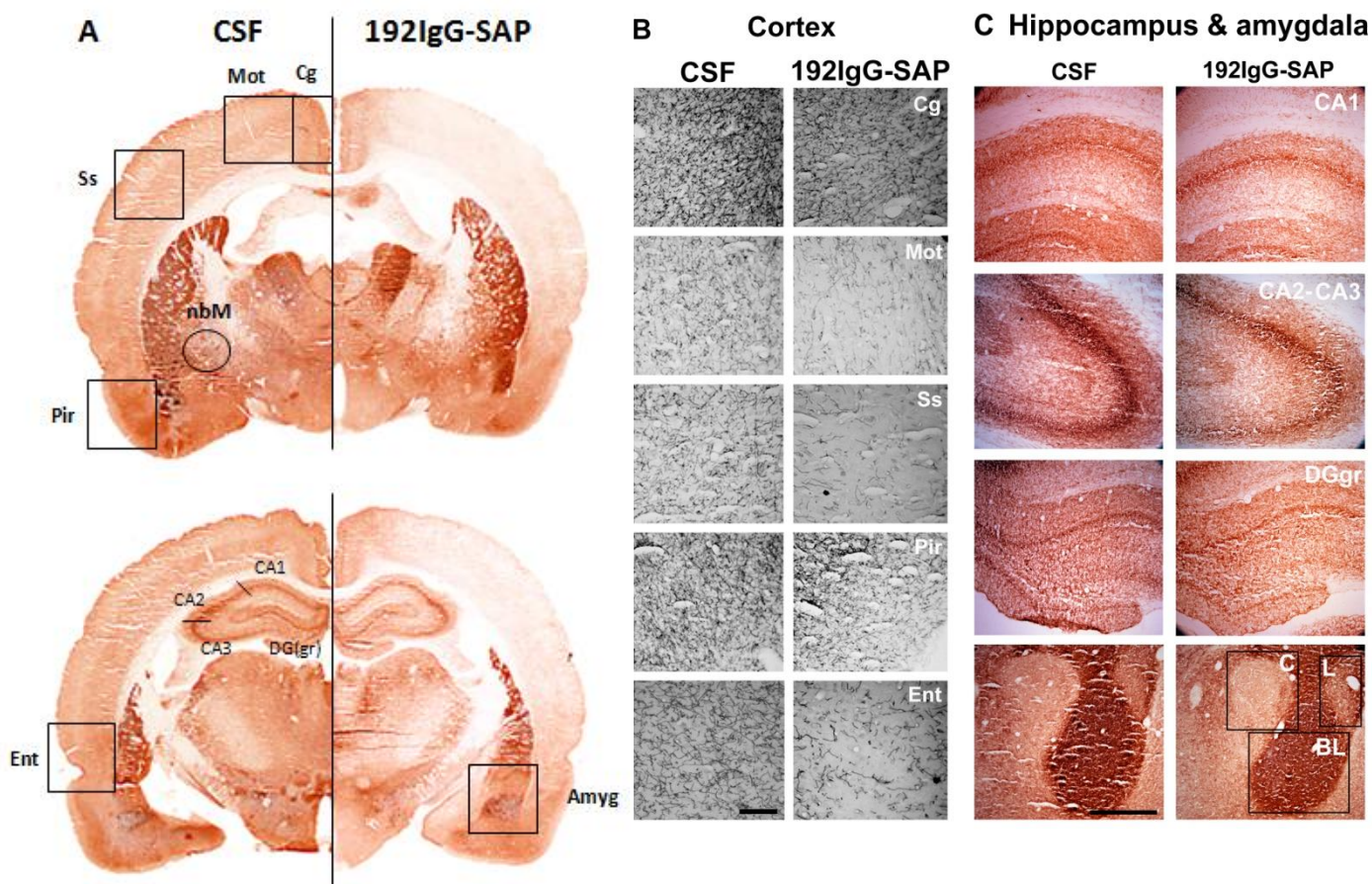


Figure 5: Histochemistry images of representative slices with AChE enzyme staining reaction corresponding to CSF (A, left) and 192IgG-SAP treated (A, right) animals. nbM (A, black circle) projection areas. (B) Cortex; Cg (cingular), Mot (motor), Ss (somatosensory), Pir (piriform), Ent (entorhinal). Scale bar = 40 μ m. (C) Hippocampus; CA1, CA2, CA3, grDG. Amygdala; C (central), L (lateral), BL (basolateral). Scale bar = 200 μ m.

4.3 Correlation between AChE⁺ neuron density and AChE activity

We observed that the loss of cholinergic neurons at the nbM induced by the specific lesion, reduced also the AChE activity at projection areas, decreasing the density of cholinergic fibers. Correlations between the number of AChE⁺ neurons (cells/mm³) and the AChE activity are represented in *Figure 6*.

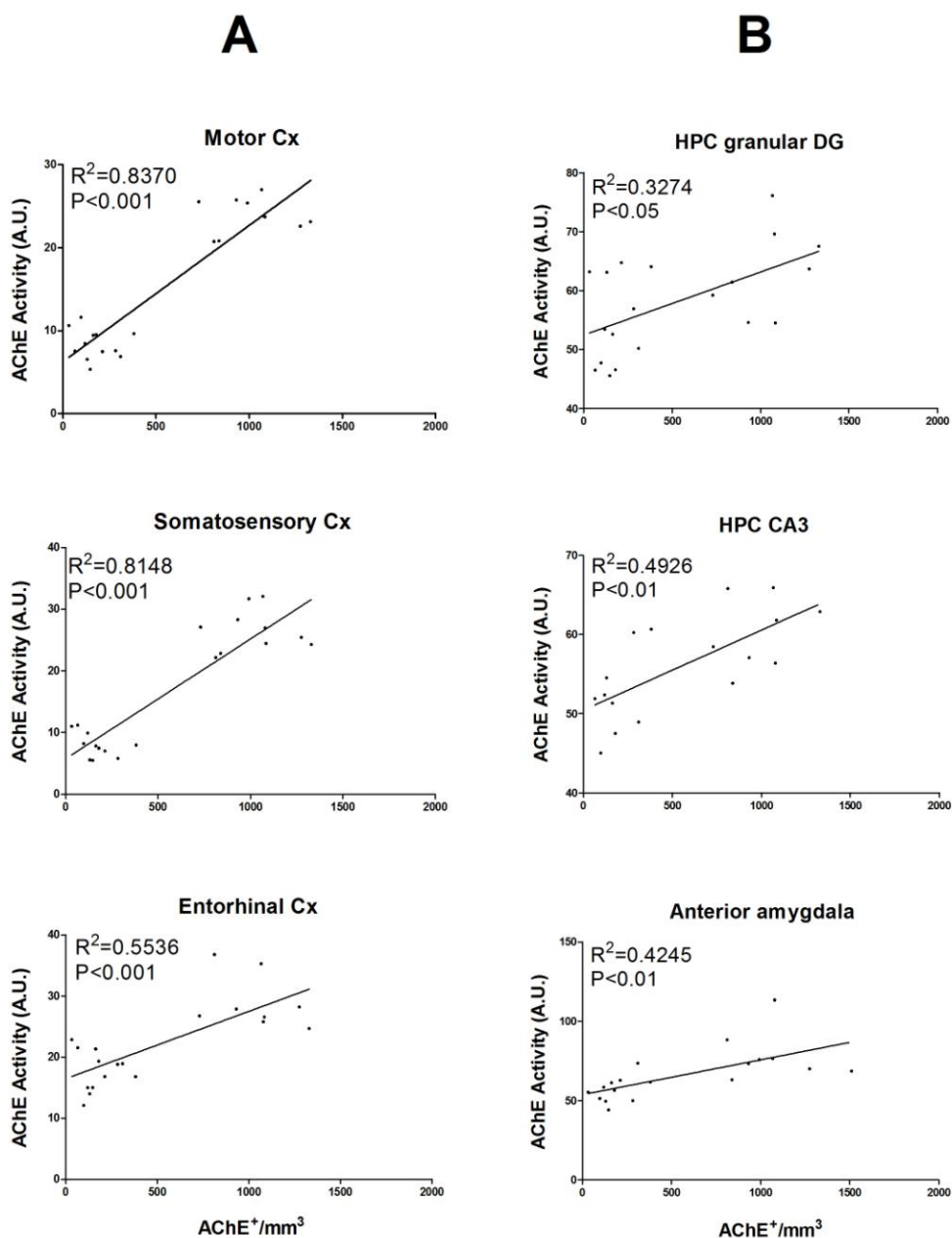


Figure 6: Correlations between AChE⁺ cells in the nbM and AChE activity in cortical areas (A) and hippocampal and amygdaloid subareas (B). R^2 , Pearson's correlation test.

5. Discussion

The present study shows that the bilateral injection of 130 ng of 192IgG-saporin intraparenchymally eliminates around the 80% of AChE⁺ neurons at the nbM inducing also a significant decrease in the density of AChE⁺ fibers at several cortical, hippocampal and amygdaloid areas. Previous studies have also reported a concomitant loss of nbM neurons and cortical ACh levels. This nbM provides the major cholinergic innervation to the frontal, prefrontal, and parietal areas of the cerebral cortex [19, 20] and the decrease in cortical ACh levels is associated with cognitive impairments [21]. Moreover, recent experiments in animal models have established that cortical cholinergic function is essential for the acquisition of new memory revealing the importance of the nbM cholinergic neurons in the formation of memory [22]. It has also been reported that the nbM sends substantial cholinergic projections to the amygdala which is related to emotions such as fear and anxiety. Therefore, the loss of nbM neurons could be related with some neuropsychiatric symptoms such as anxiety seen in AD patients. Nevertheless, the hippocampal cholinergic innervation comes mainly from the medial septum rather than from the nbM [20]. In the present study we have observed that the loss of cholinergic neurons at the nbM induces a decrease of AChE activity in some hippocampal areas such as the pyramidal layer of CA3 and the granular layer of the dentate gyrus. This decrease could be related to a direct innervation from a subpopulation of cholinergic neurons of the nbM or due to an indirect effect on AChE activity to compensate the decrease in the ACh levels observed in cortical and amygdaloid areas. Correlations between the AChE⁺ neuron density at the nbM and the AChE activity at the analyzed innervation areas, indicate the relevance of these pathways that control superior cognitive functions in the present model of cholinergic lesion.

Previous studies obtained similar results [15, 23]. The way of administration (intraparenchymal versus intraventricular), the concentration of immunotoxin used, the volume and the rate of infusion, the area of the administration, the projection areas analyzed, the postlesion period, the analyzed cholinergic marker or the histological staining method used are different in some way to previous studies. However, one of the most relevant improvement in our model is the use of a new type of needle to minimize the brain damage during the intraparenchymal administration.

Studies of AD patients found a substantial loss of the cholinergic neurons at the basal forebrain and cholinergic innervations to the cerebral cortex, hippocampus and amygdala. In addition, neuronal and synaptic damage is correlated with the severity of dementia [7]. Animal

models that mimic this characteristic are essential for the understanding of the mechanisms that underline neurodegenerative disorders. Since p75^{NTR} is a receptor mainly expressed at basal forebrain cholinergic neurons, the infusion of 192IgG-saporin into the basal forebrain, using an appropriate dose range to prevent nonspecific targeting, selectively eliminates cholinergic neurons and cholinergic projections. Moreover, it has been demonstrated that the administration of the immunotoxin mimics many biochemical, neuroanatomical and behavioural aspects of AD [15, 23]. In fact, the experimental damage to the nbM impairs different cognitive processes such as learning, memory and attention and provides a reliable animal model of AD [15]. Therefore, this lesion model represents a powerful tool which with study the cholinergic damage that characterize the neuropathology of AD suitable for the identification of new pharmacological targets and as an alternative for testing possible therapeutic interventions.

6. Bibliography

- [1] – **Whitehouse P, Price DL, Struble RG, Clark AW, Coyle JT, DeLong MRJ.** Alzheimer's disease and senile dementia: loss of neurons in the basal forebrain. *Science*, 1982; 215: 1237-1239.
- [2] – **Braak H, Braak E.** Neuropathological staging of Alzheimer-related changes. *Acta Neuropathol.*, 1991; 82: 239-259.
- [3] – **Kidd M.** Paired helical filaments in electron microscopy of Alzheimer's disease. *Nature*, 1963; 197: 192-193.
- [4] – **Bird TD.** Alzheimer disease overview. 2014.
- [5] – **Ferri CP, Prince M, Brayne C, Brodaty H, Fratiglioni L, Ganguli M, Hall K, Hasegawa K, Hendrie H, Huang Y, Jorm A, Mathers C, Menezes PR, Rimmer E, Sczufca M; Alzheimer's Disease International.** Global prevalence of dementia: a Delphi consensus study. *Lancet*, 2005; 366 (9503): 2112–2117.
- [6] – **Ballard C, Gauthier S, Corbett A, Brayne C, Aarsland D, Jones E.** Alzheimer's disease. *Lancet*, 2011. 377 (9770): 1019-1031.
- [7] – **DeKosky ST.** Neurobiology and molecular biology of Alzheimer's disease. *Rev Neurol.*, 2002; 35 (8): 752-760.
- [8] – **Wolf NJ.** Cholinergic systems in mammalian brain and spinal cord. *Prog in Neurobiol.*, 1991; 37: 475-524.
- [9] – **Kása P, Rakonczay Z, Gulya K.** The cholinergic system in Alzheimer's disease. *Prog Neurobiol.*, 1997; 52 (6): 511-535.

- [10] – **Baxter MG, Chiba AA.** Cognitive functions of the basal forebrain. *Curr Opin Neurobiol.*, 1999; 9: 178–183.
- [11] – **Mufson EJ, Counts SE, Perez SE, Ginsberg SD.** Cholinergic system during the progression of Alzheimer's disease: therapeutic implications. *Expert Rev Neurother.*, 2008; 8 (11): 1703-1718.
- [12] – **Jerene JW.** Biochemical, physiological, and behavioral characterizations of the cholinergic basal forebrain lesion produced by IgG-saporin. *Molecular Neurosurgery With Targeted Toxins*, 2005; 3: 31-58.
- [13] – **Book AA, Wiley RG, Schweitzer JB.** 192 IgG-saporin: I. Specific lethality for cholinergic neurons in the basal forebrain of the rat. *J Neuropathol Exp Neurol.*, 1994; 53 (1): 95-102.
- [14] – **Torres EM, Perry TA, Blockland A, Wilkinson LS, Wiley RG, Lappi DA, Dunnet SB.** Behavioural, histochemical and biochemical consequences of selective immunolesions in discrete regions of the basal forebrain cholinergic system. *Neuroscience*, 1994; 63 (1): 95-122.
- [15] – **Wenk GL, Stoehr JD, Quintana G, Mobley S, Wiley RG.** Behavioral, biochemical, histological, and electrophysiological effects of 192 IgG-saporin injection into the basal forebrain of rats. *J Neurosci.*, 1994; 14 (10): 5986: 5995.
- [16] – **Paxinos and Watson.** The rat brain in stereotaxic coordinates. 2005.
- [17] – **Karnowsky MJ, Roots L.** A “direct-coloring” thiocholine method for cholinesterase. *J Histochem Cytochem.*, 1964; 12: 219-221.
- [18] – **Broderson SH, Westrum LE, Sutton AE.** Studies of the direct coloring thiocholine method for localizing cholinesterase activity. *Histochemistry*, 1974; 40 (1): 13-23.
- [19] – **Coyle JT, Price DL, DeLong MR.** Alzheimer's disease: A disorder of cortical cholinergic innervations. *Science*, 1983; 219: 1184–1190.
- [20] – **Mesulam MM, Mufson EJ, Wainer BH, Levey AI.** Central cholinergic pathways in the rat: An overview based on an alternative cal consequences of selective immunolesions in discrete regions of nomenclature (Ch1–Ch6). *Neuroscience*, 1983; 10: 1185–1201.
- [21] – **Fibiger HC.** Cholinergic mechanisms in learning, memory, and dementia: a review of recent evidence. *Trends Neurosci.*, 1991; 14: 220–223.
- [22] – **Croxon, PL, Kyriazis DA, Baxter MG.** Cholinergic modulation of a specific memory function of prefrontal cortex. *Nat Neurosci.*, 2011; 14: 1510-1512.
- [23] – **Leanza, G, Nilsson OG, Wiley RG, Bjorklund A.** Selective lesioning of the basal forebrain cholinergic system by intraventricular 192 IgG-saporin: behavioural, biochemical and stereological studies in the rat. *Eur J Neurosci.*, 1995; 7: 329–343.